



Direct radiative effect of carbonaceous aerosols from crop residue burning during the summer harvest season in East China

Huan Yao¹, Yu Song¹, Mingxu Liu¹, Scott Archer-Nicholls², Douglas Lowe³, Gordon McFiggans³, Tingting Xu¹, Pin Du¹, Jianfeng Li¹, Yusheng Wu¹, Min Hu¹, Chun Zhao⁴, and Tong Zhu¹

¹State Key Joint Laboratory of Environmental Simulation and Pollution Control, Department of Environmental Science, Peking University, Beijing, China

²Centre for Atmospheric Science, University of Cambridge, Cambridge, UK

³Centre for Atmospheric Sciences, School of Earth, Atmospheric and Environmental Sciences, University of Manchester, Manchester, UK

⁴School of Earth and Space Science, University of Science and Technology of China, Hefei, Anhui, China

Correspondence to: Yu Song (songyu@pku.edu.cn)

Received: 23 August 2016 – Discussion started: 8 November 2016

Revised: 15 March 2017 – Accepted: 27 March 2017 – Published: 21 April 2017

Abstract. East China experiences extensive crop residue burnings in fields during harvest season. The direct radiative effect (DRE) of carbonaceous aerosols from crop residue burning in June 2013 in East China was investigated using the Weather Research and Forecasting Model coupled with Chemistry (WRF-Chem). Absorption of organic aerosol (OA) in the presence of brown carbon was considered using the parameterization of Saleh et al. (2014), in which the imaginary part of the OA refractive index is a function of wavelength and the ratio of black carbon (BC) and OA. The carbonaceous emissions from crop fires were estimated using the Moderate Resolution Imaging Spectroradiometer (MODIS) fire radiative power (FRP) product with a localized crop-burning-sourced BC-to-organic carbon (OC) ratio emission ratio of 0.27. Evaluation of the model results with in situ measurements of particulate matter with aerodynamic diameter less than 2.5 µm (PM_{2.5}) chemical composition, MODIS aerosol optical depth (AOD) detections and meteorological observations showed that this model was able to reproduce the magnitude, spatial variation and optical characteristics of carbonaceous aerosol pollution. The observed BC and OC peak concentrations at the site in Suixi, Anhui province, during the 2013 wheat burning season reached 55.3 µg m⁻³ and 157.9 µg m⁻³. WRF-Chem simulations reproduced these trends with a correlation coefficient of 0.74, estimating that crop residue burning contributed 86 and 90 % of peak BC and OC, respectively. The simulated hourly DRE from crop

residue burning at the top of atmosphere (TOA) reached a maximum of +22.66 W m⁻² at the Suixi site. On average, the simulations showed that the crop residue burning introduced a net positive DRE of +0.14 W m⁻² at TOA throughout East China, with BC from this source as the main heating contributor (+0.79 W m⁻²). The OA DRE from crop burning (-0.22 W m⁻²) was a combined effect of the positive DRE of absorption (+0.21 W m⁻²) and a stronger negative DRE of scattering (-0.43 W m⁻²). Sensitivity tests showed that the DRE of OA absorption strongly depended on the imaginary part of the OA refractive index, the BC-to-OA emission ratio from crop residue burning and the assumed mixing state of the aerosol, whereby the volume mixing treatment resulted in a higher positive DRE compared to the core-shell treatment. The BC mixing state and associated absorption enhancement during BC aging processes will be investigated in detail in future research.

1 Introduction

Carbonaceous aerosols emitted from biomass burning contributes 42 and 74 % of global black carbon (BC) and organic carbon (OC) emissions, respectively (Bond et al., 2004), playing an important role in the radiation budget system (Chung et al., 2012; Hobbs et al., 1997; Jacobson, 2014). The Intergovernmental Panel on Climate Change (IPCC) Fifth

Assessment Report estimated that BC from biomass burning introduced a global mean direct radiative forcing (DRF) of approximately +0.2 (+0.03 to +0.4) W m⁻², while that of organic aerosol (OA) from biomass burning was about the same magnitude with the opposite sign (Bond et al., 2013; Stocker, 2014). DRF is a measure of the change in direct radiative effect (DRE) relative to preindustrial conditions, defined as prior to the year 1750 AD by the IPCC. Precise computing of short-term DRE caused by carbonaceous aerosols is essential to accurate estimation of aerosol DRF and avoids the large uncertainties in estimations of preindustrial carbonaceous aerosol emissions (Bond et al., 2013). DRE could also be a more exhaustive gauge for comparisons between models and observations (Heald et al., 2014).

As a large agricultural country, China emits approximately 30–97 Gg BC and 100–463 Gg OC annually from crop residue burning in fields (Lu et al., 2011; Zhang et al., 2008; Huang et al., 2012; Zhou et al., 2017). During the summer harvest season, the contribution of crop residue burning to the total BC and OC emissions can be as high as 16 and 18 % in the winter wheat production regions of East China (Anhui, Jiangsu, Henan and Shandong provinces), respectively. Nonagricultural biomass burnings have a negligible contribution on BC and OC emissions during these periods (Song et al., 2009, 2010). Emission estimates for crop residue burning emissions can be derived from public provincial statistical data (Zhou et al., 2017), satellite burned area products (Song et al., 2010) and fire radiative power (FRP) from active fire products (Liu et al., 2015). The commonly used burned area products (e.g. MODIS MCD45A1) generally miss large quantities of field crop residue burnings due to their small size, and the emission estimation method depends on multiple parameters. FRP data shows relatively effective detection of small fires, and the corresponding emission estimation methods use fewer parameters, which further reduces the potential uncertainties in the estimates (Liu et al., 2015). To our knowledge, only one study has focused on the DRE of carbonaceous aerosol from crop-burning sources over China (Li et al., 2016), which only calculated BC DRE using the offline GEOS-Chem model, and used underestimated and coarse open biomass burning emissions (Lu et al., 2011). It is therefore important to better understand the impact of this significant source of carbonaceous aerosol on regional climate in China.

The co-emission of BC with other aerosol components such as OA, nitrates and sulfates results in multiple mixing states, complex morphology and different optical and radiative effects. For biomass burning, rather than homogeneous or external mixing, the morphology of BC cores coated by these co-emitted aerosol species is regarded as more realistic and supported by recent observations and modelling results (Liu et al., 2017; Bauer et al., 2013; Schwarz et al., 2008). This core–shell treatment was believed to amplify BC's absorption through focusing more photons as a lens by a factor of 1.5–2.0 (assuming the shell non-absorbing) than the ex-

ternal mixing state (Bond et al., 2006; Schnaiter et al., 2005; Q. Wang et al., 2014), and thus affecting the BC DRE (Jacobson, 2001).

Aside from the well-established radiative absorption of BC, which is primarily emitted from imperfect combustion sources (Chang et al., 1982), other co-emitted organic carbonaceous aerosol have been found to have an absorptive component closely linked to biomass burning (Kirchstetter et al., 2004; Lack et al., 2012). These are commonly called brown carbon aerosol (Andreae, 1995) and contribute a global positive mean radiative forcing of +0.1 to +0.25 W m⁻² by absorption (Feng et al., 2013). OA radiation absorption is characterized by a strong dependence on wavelength, increasing sharply from shortwave-visible to ultraviolet ranges (Andreae and Gelencsér, 2006; Bond, 2001). The light absorption of OA from different sources is also highly variable. For biomass burning, the temperature of the combustion process, moisture content and fuel type can be factors, complicating the treatment of OA absorption in models (Laskin et al., 2015). Therefore, studies which use constant optical parameters of OA absorption for climate forcing calculations have significant associated uncertainties (Feng et al., 2013; X. Wang et al., 2014). Recently, Saleh et al. (2014) proposed that the absorptivity of OA from biomass burning, both fresh and aged, could be parameterized as a function of the BC-to-OA ratio. This parameterization has been used to simulate the DRE of OA absorption from biomass or biofuel burning emissions globally in several studies (Kodros et al., 2015, 2016; Saleh et al., 2015). More recent research has suggested that the increased absorption of biomass burning aerosol particles, interpreted by Saleh et al. (2014) as being due to OA absorptivity, could be interpreted as enhanced BC absorption from the mixing state of the aerosol (Liu et al., 2017). However, we will be using the theoretical framework that Saleh et al. (2014) provide for this paper.

The offline models used in the previous studies investigating warming due to OA absorption (e.g. GEOS-Chem) probably have induced errors from the inconsistencies in space, time and physical parameterizations between the separated atmospheric, meteorological and chemical transport components. These errors could be circumvented in online models by integrating the chemical modelling into the meteorology simulation. Online models, such as the Weather Research and Forecasting Model coupled with Chemistry (WRF-Chem; Fast et al., 2006; Grell et al., 2005), could provide further insight into aerosol–cloud–radiation feedbacks, which are crucial for understanding climate change (Zhang, 2008) but ignored in offline models. WRF-Chem contains the physics to simulate the aerosol DRE but needs extra radiation diagnostics to distinguish the DRE from other aerosol–radiation–cloud interactions. Both Huang et al. (2015) and Zhao et al. (2013) calculated the aerosol DRE in WRF-Chem by performing calculations of aerosol optical properties and radiative transfer multiple times with and without one aerosol component and its associated water. Following

Ghan et al. (2012), Archer-Nicholls et al. (2016) calculated the DRE due to biomass burning aerosols in WRF-Chem by using double calls to the radiation driver to derive extra diagnostic variables with the refractive index of all aerosol species set to zero.

In this study, the DRE of carbonaceous aerosol from crop residue burning in East China was quantified using the online Weather Research and Forecasting Model coupled with Chemistry, using high-resolution carbonaceous aerosol emissions from crop fires calculated using a fire radiative power method (Liu et al., 2015). Sensitivity to OA absorptivity, and its variation with wavelength and BC-to-OA ratio, were tested using the Saleh et al. (2014) parameterization. Simulations were conducted for the harvest season in June 2013.

2 Methods and data

2.1 Model configuration

The online coupled meteorology–chemistry model, WRF-Chem version 3.6.1, was used for this study (Grell et al., 2005). Double-nested domains centred at 36.5° N, 115.52° E were set with the coarse domain divided into 51×59 grid cells of 75 km horizontal resolution and the fine domain divided into 48×63 grid cells of 25 km resolution (Fig. 1). The 25 vertical layers from the ground level to the top pressure level of 50 hPa were used for both domains. The global atmospheric reanalysis data ERA-Interim produced by the European Centre for Medium-Range Weather Forecasts (ECMWF) was used as the initial meteorological field and boundary conditions with 3-hourly surface parameters and 6-hourly upper-air parameters (Dee et al., 2011). The meteorology fields were initialized at the start of each model run, which covered 36 h with the first 12 h as a spinup. The total simulation time covered the entire month of June, starting from 26 May to minimize the impact from initial conditions, to cover the local harvest season of the main crop (wheat). The physical parameterizations and domain settings used are summarized in Table 1.

For gas-phase chemistry, we chose the Model for Ozone and Related chemical Tracers version 4 (MOZART-4) mechanism (Emmons et al., 2010), extended with clearer aromatic compounds and monoterpenes treatments (Knote et al., 2014). The aerosol processes, such as coagulation and thermodynamic equilibrium, were treated using the Model for Simulating Aerosol Interactions and Chemistry (MO-SAIC) scheme (Zaveri et al., 2008), in which four discrete size bins were distinguished by dry physical particle diameters (0.039–0.156, 0.156–0.625, 0.625–2.5, and 2.5–10.0 μm). Following Knote et al. (2015), we used the volatility basis set (VBS) scheme to better represent SOA formation through the oxidation of multiple biogenic and anthropogenic volatile organic compounds and subsequent gas–aerosol partitioning of semi-/intermediate volatil-

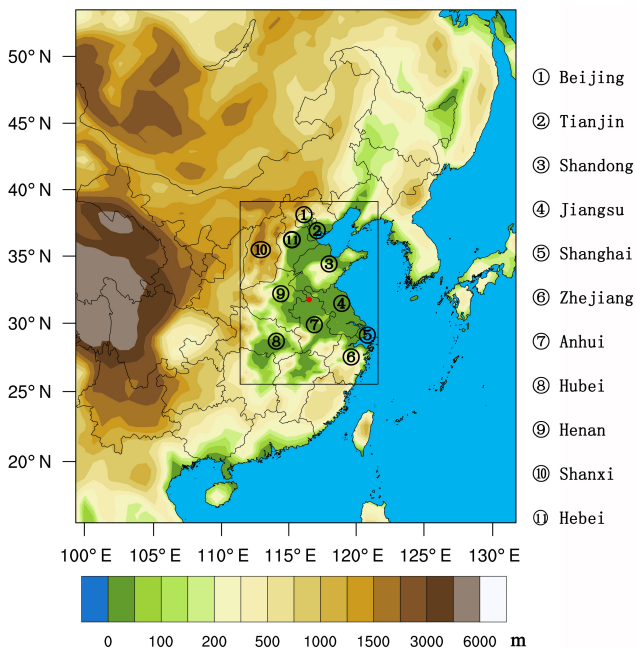


Figure 1. Double-nested Weather Research and Forecasting Model (WRF) modelling domains and topographic field (m); the sampling site (Suixi) is indicated by the red dot.

Table 1. WRF-Chem configuration options and settings.

Configuration options	
Radiation	RRTMG short- and longwave
Cumulus parameterization	New Grell scheme (G3)
Land surface	Noah
Microphysics	Lin et al. (1983)
Photolysis	Fast-J
Gas chemistry	MOZART-4
Aerosol chemistry	MOSAIC
Boundary layer	Yonsei University
Domain settings	
Horizontal grid	52 \times 60 (coarse) ; 49 \times 64 (fine)
Grid spacing	75 km \times 75 km (coarse); 25 km \times 25 km (fine)
Vertical layers	25
Projection	Lambert conformal conic

ity organic compounds (SVOC/IVOC). Direct emissions of SVOC/IVOC were not considered in this scheme.

To distinguish the aerosol effect on radiation budget directly by absorbing and scattering from other aerosol–radiation–cloud interactions, we added diagnostic calls to the radiation driver, following Archer-Nicholls et al. (2016) and Ghan et al. (2012). “Clean-sky” diagnostic variables (e.g. SW_{cln}), defined as what the net radiative fluxes at the top and bottom of the atmosphere would be if there were no aerosol in the column, were calculated by calling the radi-

ation driver with the complex refractive index of all aerosol species set to zero. Thus, the clean-sky variables include the radiation scattering and absorbing effects of clouds but ignore all aerosol radiation scattering and absorption. The DRE of all the aerosol species (ADRE) at the top of atmosphere (TOA) can be diagnosed by the difference of all-sky (including all the aerosol–radiation–cloud interactions) and clean-sky shortwave irradiances at TOA:

$$\text{ADRE} = (\text{SW}_{\text{TOA}}^{\downarrow} - \text{SW}_{\text{TOA}}^{\uparrow}) - (\text{SW}_{\text{TOA,cln}}^{\downarrow} - \text{SW}_{\text{TOA,cln}}^{\uparrow}), \quad (1)$$

where $\text{SW}_{\text{TOA}}^{\downarrow}$ and $\text{SW}_{\text{TOA}}^{\uparrow}$ represent the shortwave radiation fluxes in the down and up direction at TOA, respectively. The DRE estimates of crop residue burning and the related carbonaceous aerosols were then determined from the ADRE differences between scenarios (further explained in Sect. 2.4). Taking advantage of the multiple scattering capability, and taking computational speed and accuracy into consideration, the rapid radiative transfer model (RRTMG; Mlawer et al., 1997) was selected to simulate shortwave flux change.

Aerosol optical properties, including absorption efficiency, scattering efficiency and the asymmetry parameter, are necessary for aerosol radiative transfer calculations. In this study, these three parameters were computed by the core-shell Mie theory for each bin (Ackerman and Toon, 1981) and then determined by summation over all size bins (Fast et al., 2006). The spherical core–shell configuration calculates aerosol optical properties by assuming the BC core is coated with a homogeneously mixed shell of other species. For each bin, the complex refractive index of the shell was derived by volume averaging that of all non-BC species (Barnard et al., 2010). By default, the imaginary refractive index of OA in WRF-Chem is zero. In this study, we adopted the Saleh et al. (2014) parameterization to calculate the OA absorptivity, based on smog chamber experiments for both fresh and chemically aged emissions from globally important fuels to characterize the effective absorptivity of organic aerosols as a function of the ratio of BC to OA. This parameterization has previously been incorporated into the 3-D global chemical transport model GEOS-Chem to calculate global direct radiative effect of carbonaceous aerosols emitted from biomass and biofuel burning (Saleh et al., 2015; Kodros et al., 2015, 2016). According to the parameterization, the imaginary part of OA's refractive index, k_{OA} , can be estimated from the ratio of BC to OA from biomass burning as follows:

$$k_{\text{OA},550} = 0.016 \log_{10} \left(\frac{\text{BC}}{\text{OA}} \right) + 0.04, \quad (2)$$

$$\omega = \frac{0.21}{\left(\frac{\text{BC}}{\text{OA}} + 0.07 \right)}, \quad (3)$$

$$k_{\text{OA}} = k_{\text{OA},550} \left(\frac{550}{\lambda} \right)^{\omega}, \quad (4)$$

where $k_{\text{OA},550}$ is the imaginary part of OA's refractive index at a wavelength (λ) of 550 nm and ω is the wavelength dependence of k_{OA} .

2.2 Emission inventory

The crop residue burning emissions were derived based on a fire radiative power method (Liu et al., 2015), which reduces uncertainties and captures more crop fires than the MODIS (Moderate Resolution Imaging Spectroradiometer) burned area products (Roy et al., 2008). The daily emissions product based on the FRP method has a 1 km horizontal resolution. The crop-burning-sourced BC and OC emissions in this study were 4.3 and 15.9 Gg during the month of June, 2013, close to those in GFEDv4.1 data in June of 2013 (2.7 and 8.4 Gg for BC and OC, respectively; Randerson et al., 2012) and the results derived from agricultural statistics data in June of 2006 (6.7 and 20.7 Gg for BC and OC, respectively; Huang et al., 2012). The diurnal allocation of the emissions was based on previous household surveys (Fig. S1, more detail could be found in the Supplement).

The BC and OC emission factors from crop fires in this study (0.54 and 1.98 g kg⁻¹, respectively) were set specifically for winter wheat residue burning in East China. It was averaged using published emission factors calculated from winter wheat combustion experiments in the field and laboratory (Hays et al., 2005; Li et al., 2007; Dhammapala et al., 2007; Turn et al., 1997). The BC-to-OC ratio from crop burning was 0.27, falling within the range of 0.20–0.32 observed during harvest seasons in East China (Li et al., 2014; Yamaji et al., 2010; Yang et al., 2008). Note that when inputted into WRF-Chem, the OA emissions were calculated by multiplying OC emissions by a factor of 1.4 to account for the associated hydrogen and oxygen mass making up total OA. The simulated primary and secondary OC concentrations were calculated by dividing the simulated OA fields by factors of 1.4 and 1.8, respectively (Gilardoni et al., 2009).

The Multi-resolution Emission Inventory for China (MEIC, see <http://www.meicmodel.org/dataset-meic.html>) database was applied for China, and the Mosaic Asian Anthropogenic Emission Inventory (MIX, see <http://www.meicmodel.org/dataset-mix.html>) database (Li et al., 2017) was applied for the surrounding countries, providing power plant, industrial, residential, and vehicle emissions. Biogenic emissions were calculated online using MEGAN (Model of Emissions and Gases from Nature; Guenther, 2006), and dust emissions were not included in our study.

2.3 In situ measurements and other data

Particulate matter with aerodynamic diameter below 2.5 µm (PM_{2.5}) chemical components were sampled and analysed from 30 May to 27 June 2013 at the site (33°54'37'' N, 116°45'46'' E) in Suixi, Anhui province, China, a location close to vast stretches of wheat fields, the nearest of which was only

1 km away. There were two sampling periods each day: from approximately 07:40 (GMT+8.0) to 18:00 and from 18:40 to 07:00 the next morning. BC and OA were measured using a thermal/optical carbon analyzer (Sunset Laboratory, Tigard, OR, USA) with quartz fiber filters. More complete detail on sampling and analysis can be found in Li et al. (2014).

The MODIS Level-2 Atmospheric Aerosol Product (04_L2) data (Collection 6), at a 1 km daily resolution for June 2013, was used to evaluate the aerosol optical depth (AOD) simulations, with the Deep Blue algorithms (Hsu et al., 2006) integrated with the existing MODIS algorithm to retrieve AOD over the entire land area, including both dark and bright surfaces.

2.4 Numerical Experiments

Six parallel simulations were conducted to investigate the DRE of carbonaceous aerosols from crop residue burning as well as the OA absorption (Table 2). The BASE simulation included all emissions, assumed BC cores were coated by shells of all other well-mixed aerosol species for optical calculations and parameterized the OA absorption based on Saleh et al. (2014). The crop residue burning DRE was estimated by diagnosing the ADRE difference between the BASE and nCB runs. To further compute the DRE from BC and OA from crop residue burning, we conducted two more parallel simulations without the corresponding BC and OA emissions (i.e. nBCCB and nOACB, respectively). Since the parameterization of Saleh et al. (2014) was applicable for the OA from biomass burning, the DRE calculation of OA absorption from crop residue burning (DRE_{OACB_ABS}) should exclude the absorption of OA from other sources. To evaluate the impact of radiatively absorbing OA, two simulations (nOAABS and nOACB_nOAABS) were conducted with the imaginary part of the OA refractive index set to zero. Thus, the direct radiative effect of absorbing OA from crop residue burning (DRE_{OACB_ABS}) was given by

$$DRE_{OACB_ABS} = (ADRE_{BASE} - ADRE_{nOAABS}) - (ADRE_{nOACB} - ADRE_{nOACB_nOAABS}). \quad (5)$$

3 Results and discussion

3.1 Model evaluation

The meteorological fields from the BASE simulation were evaluated by comparison with temperature and relative humidity at 2 m above ground surface (T2 and RH2, respectively) and wind speed and direction at 10 m above ground (WS10 and WD10) measurements from 221 matched land-based stations in East China. Statistical indices (Table 3), including mean bias (MB), root-mean-square error (RMSE), fractional bias (FB), fractional error (FE) and index of agreement (IOA), indicated that the model well-simulated both

temporal variations and spatial distributions of the four meteorological fields. The model well-reproduced the T2 and RH2, with IOAs of 0.92 and 0.87, respectively. The statistical indices of T2 had a slightly better coincidences than those of RH2, with the RMSE of RH2 reaching 13.93. There was a small underestimation (-0.69%) of RH2, while WS10 was slightly overestimated (0.99 m s^{-1}). At three typical sites (Fuyang, Yanzhou and Xuzhou) corresponding to the three main districts affected by crop fire (mentioned below), the model captured the general temporal trends of T2 and RH2, although the RH2 was slightly underestimated (Fig. S2), which might have led to small differences in certain aerosol physical properties (Chapman et al., 2009; Xia et al., 2007). In general, the simulation results were comparable to the meteorological observations.

The temporal variation of fire counts detected by MODIS in East China in June 2013 is shown in Fig. 2a. Approximately 97 % of the fire counts occurred from 1–21 June, while the fire counts decreased to < 200 per day thereafter. Throughout the rest of this study, we focus on the summer harvest period from 1–21 June. The areas of intense burning moved from inland to coastland and from the south to the north over time in three phases, corresponding to the harvest time regulation and tied to the summer air temperature differences between the marine and continental climate, and low and high latitude. The districts most affected by crop residue fires were the southeastern Henan and central Anhui provinces from 1–8 June, the northern Anhui province from 9–16 June, and the northern Jiangsu and eastern Shandong provinces from 17–21 June (Fig. 2b).

As shown in previous studies (Yang et al., 2008; Li et al., 2014), crop residue burning led to the deterioration of local air quality, particularly affecting carbonaceous aerosol surface concentrations. At the Suixi site, BC and OC surface concentration observations fluctuated smoothly with values < 10 and $20 \mu\text{g m}^{-3}$ in early June, respectively, and then began to increase on the night of 12 June, reaching peaks on the nights of 13–15 June with mean values of 55.3 and $157.9 \mu\text{g m}^{-3}$, respectively (Fig. 3a and b). The peak value of observed OC was about three times that of observed BC, close to the BC-to-OC ratio of crop residue burning emissions used in the model (0.27, in Sect. 2.2), indicating that the dominant source of carbonaceous aerosols pollution was local biomass burning. WRF-Chem well-reproduced the carbonaceous aerosols concentrations fluctuating trends (Fig. 3a and b), with a correlation coefficient of 0.74 (Fig. 3c and d). The comparison between BASE and nCB scenarios revealed that crop residue burning contributed 86 and 90 % to the BC and OC concentrations respectively during the highest peaks (13–15 June). Our simulated carbonaceous aerosol contributions from crop burning (74.7 % for BC and 81.2 % for OA) at the Suixi site from 12–17 June were consistent with the positive matrix factorization results (74.5 % for BC and 75.8 % for OA) measured during the same period (Li et al., 2014). Over East China, the simulated crop residue burn-

Table 2. Descriptions of the main simulations.

Simulation	Emission inventory	BC-to-OC ratio	OA absorptivity	Mixing state
BASE	Comprehensive	0.27	Saleh et al. (2014)	Core–shell
nCB	No crop residue burning emissions	0.27	Saleh et al. (2014)	Core–shell
nBCCB	No BC emissions from crop residue burning	0.27	Saleh et al. (2014)	Core–shell
nOACB	No OA emissions from crop residue burning	0.27	Saleh et al. (2014)	Core–shell
nOAABS	Comprehensive	0.27	None	Core–shell
nOACB_nOAABS	No OA emissions from crop residue burning	0.27	None	Core–shell

Table 3. Statistical analyses of the simulated meteorological variables versus the ground observations. MB, mean bias; RMSE, root-mean-square error; FB, fractional bias; FE, fractional error; IOA, index of agreement.

Index	MB ^a	RMSE ^b	FB ^c	FE ^d	IOA ^e
2 m temperature (°)	0.26	2.72	0.01	0.09	0.92
2 m relative humidity (%)	-0.69	13.93	-0.02	0.16	0.87
10 m wind speed (m s ⁻¹)	0.99	2.01	0.45	0.65	0.61
10 m wind direction (°)	7.32	56.03			

$$^a \text{MB} = \frac{1}{N} \sum_{i=1}^N (\text{sim}_i - \text{obs}_i), \quad ^b \text{RMSE} = \sqrt{\frac{1}{N} \sum_{i=1}^N (\text{sim}_i - \text{obs}_i)^2 / N}$$

$$^c \text{FB} = 2\sqrt{(\text{sim}_i - \text{obs}_i)/(\text{sim}_i + \text{obs}_i)}/N, \quad ^d \text{FE} = \sqrt{|\text{sim}_i - \text{obs}_i|/(\text{sim}_i + \text{obs}_i)^2}/N$$

$$^e \text{IOA} = 1 - \frac{N \times \text{RMSE}^2}{\sum_{i=1}^N (|\text{obs}_i - \overline{\text{obs}}| + |\text{sim}_i - \overline{\text{obs}}|)^2}, \text{ where the term sim and obs refer to the simulated and observed meteorological values, respectively, and } N \text{ represents the number of data pairs.}$$

ing contribution to the total OC mass concentration of 37.6 % was also in agreement with the previous observed range of 24–67.5 % from sites in the same district (Fu et al., 2012; Li et al., 2014). The time variations of ammonium, sulfate and nitrate in PM_{2.5} were also well-reproduced and had more fluctuation than that of carbonaceous aerosols, indicating a weaker correlation with the crop fires (Fig. S3).

The Suixi site was almost unaffected by the intensive fire counts in southeastern Henan and central Anhui from 1–8 June, owing to the prevailing southeast wind, which instead transported the pollutants to Henan, Shanxi and the southern Hebei province (Fig. 4a). The peak values of carbonaceous aerosols at the Suixi site were centralized around 12–16 June, corresponding to the high fire counts in northern Anhui during this period (Fig. 2). Most of the North China Plain witnessed more than 15 µg m⁻³ BC and 30 µg m⁻³ OC due to the local crop residue burning as well as the pollutants carried by the south wind. After 17 June, the main burning area moved east to the northern part of the Jiangsu province, impacting Shandong province whilst having less influence in Suixi. The main body of carbonaceous aerosol pollution during the summer harvest moved from south to north and from inland to coastal areas (Fig. 4), corresponding to the shifts in fire count distribution. Carbonaceous aerosol surface concentrations increased rapidly in the evening at around 19:00–20:00 (GMT+8.0) and reached peak values at dawn (05:00–06:00, GMT+8.0), due to the relatively looser management

of crop burning and weaker boundary layer mixing at night-time. After sunrise, the concentrations gradually decreased as the fires slowly extinguished and the surface inversion coupled to layers aloft enhanced vertical mixing (Cao et al., 2009).

The 550 nm AOD detected by MODIS was well-reproduced by WRF-Chem (Fig. 5a and b), showing high values (above 1) in the North China Plain and Jinagsu, consistent with the MODIS agricultural fire counts distribution during the summer harvest in Fig. 2. Higher AODs in megacities, including Beijing, Shanghai and Tianjin, might be attributable to the increased sulfate and ammonium concentrations and scattering in summer (Huang et al., 2015). We calculated the AOD at 550 nm from that at 400 and 600 nm using the Ångström exponent, as aerosol optical properties were computed only at four wavelengths in the model (Nordmann et al., 2014). The MODIS AOD data around 23 sites were matched with the simulated AOD by hour, showing a normalized mean deviation of -16.1 % and a correlation coefficient (*R*) of 0.52 (Fig. S4). This small underestimation might be partly caused by the underestimation of the summer RH (Yoon and Kim, 2006). Several studies have also noted that the MODIS retrieval AOD showed high bias compared with ground-based measurements such as the Aerosol Robotic Network (AERONET) data (Huang et al., 2015; Myhre et al., 2009; Zhao et al., 2013).

Table 4. The DRE differences (W m^{-2}) between the cases at TOA during the summer harvest (1–21 June) in 2013.

BASE – nCB	BASE – nBCCB	BASE – nOACB	(BASE – nOAABS) – (nOACB – nOACB_nOAABS)
+0.14 W m^{-2}	+0.79 W m^{-2}	-0.22 W m^{-2}	+0.21 W m^{-2}

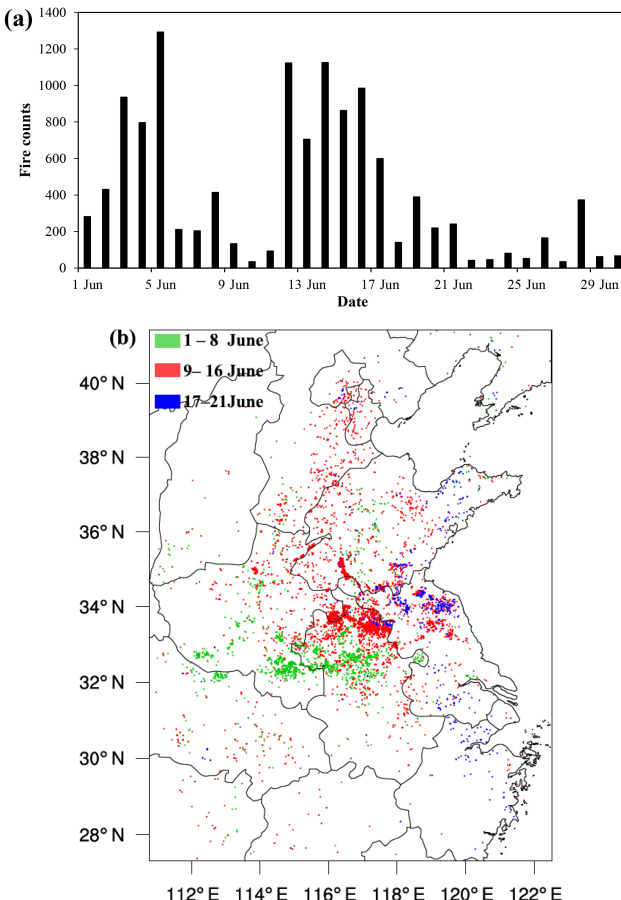


Figure 2. (a) Time series of the fire counts detected by the Moderate Resolution Imaging Spectroradiometer (MODIS) in East China in June 2013. (b) Spatial distribution of MODIS agricultural fire counts in East China in June 2013. The green, red and blue dots represent the location of fire counts detected in 1–8, 9–16 and 17–21 June, respectively.

Aerosol absorption optical depth (AAOD) is defined as the AOD multiplied by the solar absorption potential (i.e. $1 - \text{single scattering albedo}$), giving a measure of the radiation absorbed by aerosol in the column. Similar patterns can be seen between the spatial distribution of 550 nm AAOD and the carbonaceous aerosols concentration during the summer harvest (Fig. 5c and d), especially at the corner of Henan, Anhui, Jiangsu and Shandong provinces. Because of the relatively short atmospheric lifetimes of BC and OA, the highest surface concentrations and high AAOD could be found close to the regions where crop burning was taking place

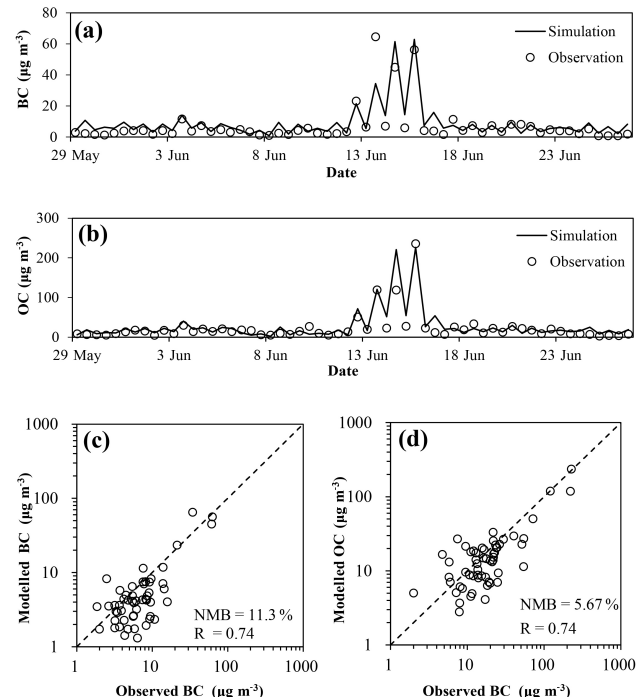


Figure 3. Time series of the observed (dots) and simulated (line) (a) black carbon (BC) and (b) organic carbon (OC) mass concentrations ($\mu\text{g m}^{-3}$) at the Suixi site. Scatterplots of simulated (c) BC and (d) OC mass concentrations ($\mu\text{g m}^{-3}$) and the corresponding observed values. NMB and R represent normalized mean bias and correlation coefficient, respectively.

(Bond et al., 2013; Laskin et al., 2015; Zhuang et al., 2011). It is worth noting that we treat all-source OA as absorbing aerosol, thus artificially amplifying the AAOD from anthropogenically emitted OA, particularly around the megacities of Beijing and Tianjin. Additionally, the core–shell mixing assumption might also lead to higher AAOD in contrast to the externally mixing assumption due to absorption enhancement of BC-contained particles in these megacities (Liu et al., 2017).

3.2 Direct radiative effect of crop residue burning

Calculated as the ADRE difference between the BASE and nCB simulations, a mean positive DRE of $+0.14 \text{ W m}^{-2}$ was introduced by crop residue burning at TOA in East China during the summer harvest (Table 4). This is higher than previous cooling-to-neutral DRE estimations of open biomass burning (Abel et al., 2005; Archer-Nicholls et al., 2016;

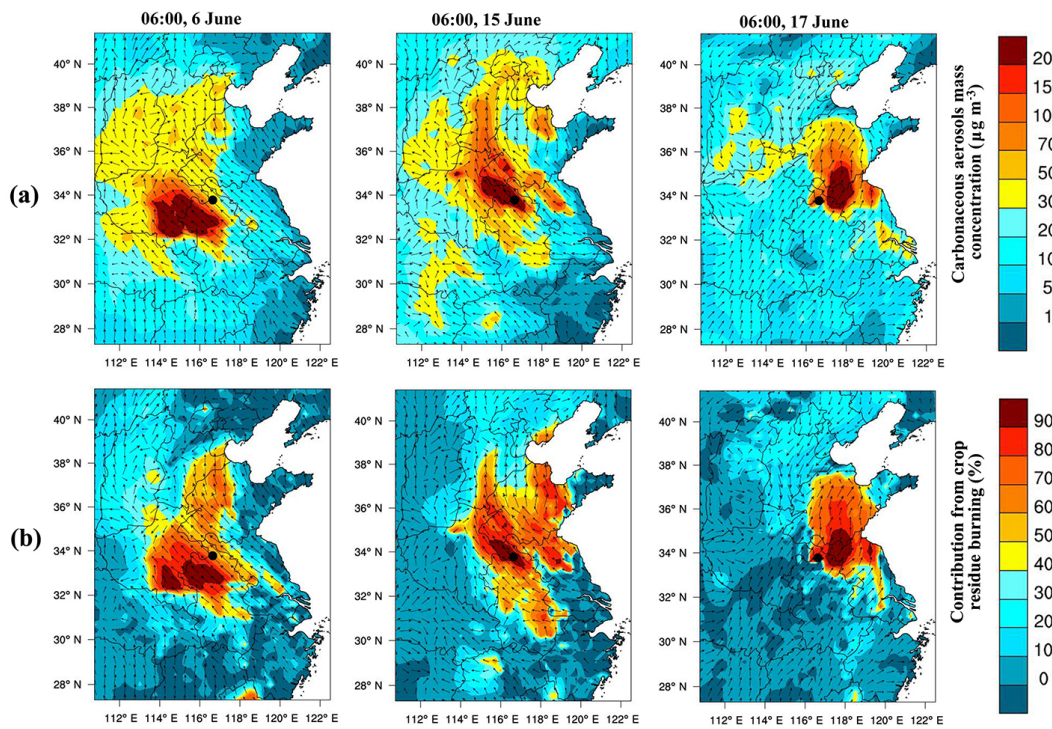


Figure 4. Spatial distributions of (a) carbonaceous aerosols mass concentration ($\mu\text{g m}^{-3}$) at the lowest model level ($\sim 20\text{ m}$) and (b) its contribution from crop residue burning (%) in the three typical hours (06:00, GMT+8.0) during the summer harvest (1–21 June) in June 2013. The location of the sampling site (Suixi) is indicated by the black dot. The arrows represent the surface ($\sim 20\text{ m}$) wind fields.

Sakaeda et al., 2011; Chung et al., 2012; Myhre et al., 2013), which might be attributed to the incorporation of the OA absorptivity scheme of Saleh et al. (2014) in this study (Kodros et al., 2015, 2016; Saleh et al., 2015). The spatial distribution of crop residue burning DRE (Fig. 6a) shows similar patterns to that of the mean carbonaceous aerosols concentration, providing further evidences that the carbonaceous aerosols emitted from crop residue burning were the dominant contributors to the DRE. Positive DRE values mainly appeared in the North China Plain, and higher ones (more than 0.5 W m^{-2}) were in eastern Henan, southwestern Shandong, northern Jiangsu and northern Anhui provinces. At the Suixi site, the hourly DRE at TOA from crop residue burning reached a peak of $+22.66\text{ W m}^{-2}$ at 13:00 on 15 June (GMT+8.0).

The DRE of BC from crop residue burning was calculated to be $+0.79\text{ W m}^{-2}$ at TOA during the summer harvest based on the difference between the BASE and nBCCB simulations. This is higher than the DRE estimation from biomass-burning-sourced BC ($+0.1$ to $+0.5\text{ W m}^{-2}$) in East China for the summer of 2010 by Li et al. (2016), which used an offline model with a coarse resolution. The emission inventories they used might have also underestimated BC emissions from open biomass burning, especially during the harvest season or in the burning zone, due to the traditional estimation methods and spatial allocation rules (Lu et

al., 2011). Moreover, the external mixing state that they used would lead to lower and less accurate DRE estimations in contrast to the core–shell treatment (Jacobson, 2001). After dividing the DRE of BC from crop residue burning by the corresponding source contribution to the BC mass concentration (17.6 %), our all-source BC DRE estimate at TOA for the summer harvest of $+4.5\text{ W m}^{-2}$ was lower than the national all-sky averaged anthropogenic BC DRE for the summer of 2006 ($+5\text{ W m}^{-2}$; Huang et al., 2015) and BC DRE in East China for the summer of 2008 ($+5$ to $+15\text{ W m}^{-2}$; Gao et al., 2014). It was worth noting that these previous studies adopted the volume mixing treatment, which would overestimate the BC DRE. Further, the neglect of crop residue burning emissions in Gao et al. (2014) might cause an underestimation. Normalized DRE, defined by Boucher and Anderson (1995) (and first used in Feichter et al., 1997) as the ratio of the forcing to the aerosol mass burden, was calculated to isolate the differences in the aerosol column burden from the differences in all other model processes that lead to carbonaceous aerosols radiative forcing (Bond et al., 2013). Our calculated normalized DRE with respect to the BC burden from crop residue burning was $+941.33\text{ W g}^{-1}$, within the existing estimated global normalized DRF ranges of $+870$ to $+2730\text{ W g}^{-1}$ (Bond et al., 2013; Ramanathan and Carmichael, 2008; Schulz et al., 2006). Figure 6b illustrates that the high values of BC DRE (above $+2.0\text{ W m}^{-2}$)

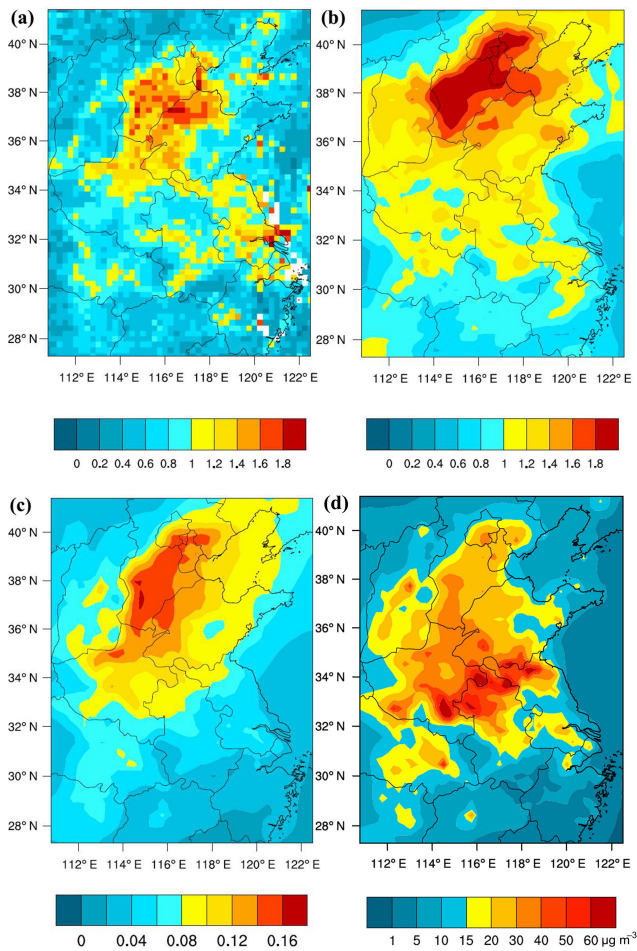


Figure 5. Spatial distribution of mean (a) 550 nm aerosol optical depth observations from MODIS, (b) 550 nm aerosol optical depth from WRF-Chem, (c) mean absorption aerosol optical depth from WRF-Chem and (d) mean carbonaceous aerosol concentration ($\mu\text{g m}^{-3}$) at the lowest model level ($\sim 20 \text{ m}$) during the summer harvest (1–21 June). BASE run is shown.

during the summer harvest mainly appeared in the western Shandong province, the Tianjin municipality, eastern Henan province, northern Anhui and northern Jiangsu provinces, similar to the spatial features of $> 20 \mu\text{g m}^{-3}$ carbonaceous aerosol mass concentration (Fig. 5d). The hotspot was in the north of the intensive-crop-fire-affected area (Fig. 2b), as the dominant southeastern wind in June transported carbonaceous aerosol to the north (Sect. 3.1). With the carbonaceous aerosols mass concentration exceeding $30 \mu\text{g m}^{-3}$, the junction of Anhui, Shandong, Henan and Hebei provinces witnessed the highest BC DRE in our domain of over $+3.0 \text{ W m}^{-2}$. The local DRE in the crop residue burning districts during intense burning periods were higher than spatiotemporally averaged estimates. Taking the Suixi site as an example, the hourly DRE of crop-residue-burning-sourced BC reached $+63.40 \text{ W m}^{-2}$ on 15 June.

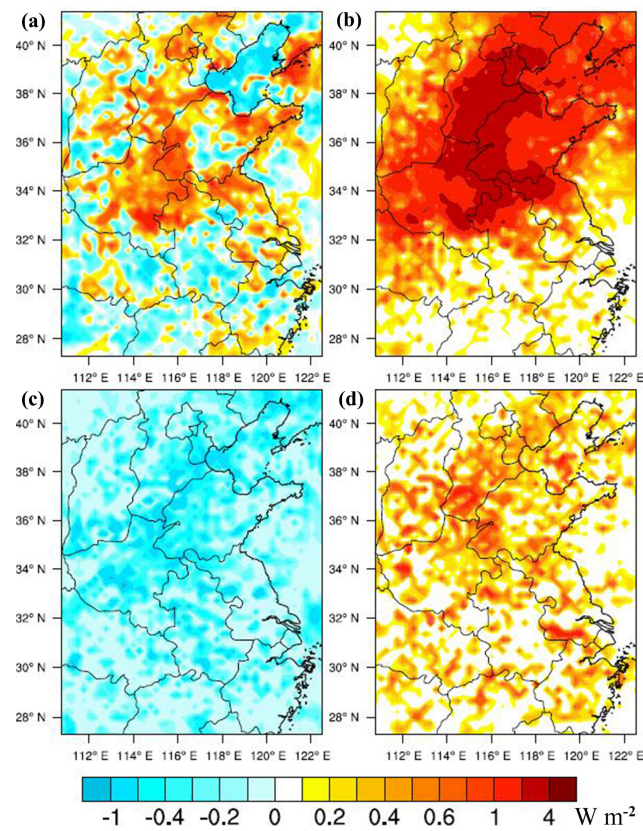


Figure 6. Spatial distribution of simulated direct radiative effect (DRE) introduced by (a) all aerosol from crop residue burning and (b) BC from crop-burning, (c) OA from crop burning and (d) the absorbing component of OA from crop-burning emissions, calculated from WRF-Chem simulations during the summer harvest (1–21 June).

By subtracting the ADRE at TOA of nOACB from that of BASE, we obtained an OA DRE from crop residue burning of -0.22 W m^{-2} in East China during the summer harvest. The normalized DRE of OA from crop residue burning, -11.46 W g^{-1} , was of smaller magnitude than existing estimates of -24 to -198 W g^{-1} (Bond et al., 2013; Ramanathan and Carmichael, 2008; Schulz et al., 2006). This positive discrepancy can be attributed to the consideration of OA absorptivity in this study. The positive DRE of OA absorption from crop residue burning was calculated to be $+0.21 \text{ W m}^{-2}$ according to the ADRE comparison among BASE, nOACB, nOAABS and nOACB_nOAABS scenarios (Sect. 2.4), in contrast to the negative DRE (-0.43 W m^{-2}) of OA scattering. The DRE of OA absorption during the summer harvest in East China in our study was within the global annual mean DRE ranges of OA absorption, of $+0.04$ to $+0.57 \text{ W m}^{-2}$ (Feng et al., 2013; Saleh et al., 2015; Q. Wang et al., 2014), and higher than the estimates in East Asia for the spring of 2011, of $+0.1$ to $+0.2 \text{ W m}^{-2}$ (Park et al., 2010). Feng et al. (2013) estimated an upper limit of annual mean DRE of OA absorption to be $+0.25$ to $+0.5 \text{ W m}^{-2}$.

in East China. The DRE of OA absorption from crop residue burning accounted for 21 % of the corresponding DRE of carbonaceous aerosols absorption, comparable to the previous OA absorption contribution estimation of 20 % derived from AERONET observations at 550 nm (Chung et al., 2012), indicating that OA played an important role in radiation absorption during the summer harvest in East China.

Figure 6c and d show a negative DRE of OA ($<-0.2 \text{ W m}^{-2}$) and a positive DRE of OA absorption ($>0.2 \text{ W m}^{-2}$) over the North China Plain, respectively. Like the spatiotemporally averaged estimates of OA DRE and its absorbing part (-0.22 and $+0.21 \text{ W m}^{-2}$, respectively), the OA DREs in most grid cells have equal magnitude to the corresponding DRE of its absorption but show an opposite sign. This implies that the negative DRE of OA scattering is roughly double the positive DRE of OA absorption in magnitude. The consideration of OA absorption therefore reduced the negative OA DRE estimates from crop burning by half.

3.3 Uncertainty

The DRE of carbonaceous aerosols was strongly dependent on the optical properties, the uncertainties of which came from various factors, including complex refractive indices, mixing state and the morphologies of the particles. Since this study was the first to attempt to use the OA absorptivity parameterization of Saleh et al. (2014) in an online model, sensitivity experiments were conducted to investigate the response of the DRE of OA absorption to the changes in the imaginary part of OA's refractive index (k_{OA}) and the BC-to-OC emission ratio from crop residue burning. With k_{OA} raised by 50 %, the DRE of OA absorption from this source increased to $+0.27 \text{ W m}^{-2}$ (Table S2), 29 % higher than that ($+0.21 \text{ W m}^{-2}$) from default simulations. When the BC-to-OA ratio was altered to 0.18 (Li et al., 2007) and 0.42 (Hays et al., 2005) by changing the BC emission factor from crop residue burning alone with that of OA constant, the DRE of OA absorption was estimated to be $+0.33$ and $+0.13 \text{ W m}^{-2}$ (Supplement Table S2), respectively. These results indicated that the k_{OA} and the BC-to-OC emission ratio were critical for estimating DRE of OA absorption and efforts are still needed to update the BC-to-OC ratio to observations in China. More details about the sensitivity tests are presented in Table S1.

The sensitivity of BC mixing state to crop residue burning DRE was also tested by changing the standard core–shell mixing rule to a volume mixing rule. In the volume mixing treatment, crop residue burning was simulated to produce a mean DRE of $+0.23 \text{ W m}^{-2}$ during the summer harvest (Table S2), which was 64 % higher than the crop burning DRE in default runs ($+0.14 \text{ W m}^{-2}$). The single-distribution core–shell assumption was believed to be a better approximation of BC DRE (Jacobson, 2001; Bauer et al., 2013; Liu et al., 2017), and more coated particles have been observed in biomass burning aerosol (Schwarz et al., 2008), so the widely

used volume mixing assumption could introduce a discrepancy in DRE. In reality, carbonaceous aerosol mixing conditions are much more various and complicated in time and space than that described in a core–shell approach. For example, Peng et al. (2016) recently reported that BC morphology varied from fractal particles to compact particles during atmospheric aging, and BC in the two distinct stages revealed quite different absorption characteristics and climatic effects. Recent study has indicated that the absorption enhancement of BC is determined by the mass ratio of non-BC to BC species in the aerosol as an alternative interpretation to absorption by OA (Liu et al., 2017). If such a setup were used instead of the Saleh et al. (2014) parameterization, it could change the magnitude and distribution of the predicted effects. Therefore, the invariant core–shell assumption during aging that we applied might overestimate the DRE of freshly emitted BC. Matsui et al. (2013) also showed that without detailed treatment of mixing state for BC aging processes in the model, the calculated aerosol radiation absorption could be overestimated by 30–40 % in the boundary layer. Hence, it should be very important to consider the variation of mixing state for calculating optical and radiative effects of biomass burning aerosols. The spherical core–shell assumption might also amplify the absorption in cases in which the BC core position is non-central (Adachi et al., 2010). Variations in moisture and temperature conditions also complicate the mixing state of carbonaceous aerosols and the light absorptivity of OA (Liu et al., 2013; Zhang et al., 2013). Moreover, the lack of consideration of atmospheric processing of OA, such as photobleaching (Laskin et al., 2015), and the potential addition of nitrate groups (Jacobson, 1999) lead to further uncertainties.

The high-resolution emission inventory based on the MODIS FRP used here may add uncertainties to the carbonaceous aerosol mass concentrations due to uncertainties arising from the MODIS detection resolution, FRP values and the per-fire-pixel fire radiative energy calculating method (Liu et al., 2015). The VBS scheme in this study ignored SOA evolved from semi-/intermediate volatility organic compounds and likely underestimates SOA concentration.

4 Conclusion

The DRE of carbonaceous aerosols from crop residue burning in June 2013 in Eastern China was investigated using WRF-Chem. The OA effective absorptivity parameterization proposed by Saleh et al. (2014) was used. The carbonaceous aerosol emissions from crop fires were estimated based on MODIS FRP products, using a localized BC-to-OC ratio from crop burning of 0.27. In situ observations conducted in Suixi, Anhui province, during the study period were utilized to evaluate the simulation. The WRF-Chem results captured the variation of carbonaceous aerosol concentrations, show-

ing peak pollution during the period from 13–15 June. The BC and OC peak concentrations reached 55.3 and 157.9 $\mu\text{g m}^{-3}$, of which crop residue burning contributed 86 and 90 %, respectively, as derived from analysing coincident model output. The simulation results also reproduced the temperature and relative humidity from ground-based observations and MODIS-detected AODs, although there was a slight overestimation of wind speed. During the summer harvest in East China (1–21 June), similar patterns were found among simulated AAOD, fire counts detected by MODIS and carbonaceous aerosols concentrations, with higher values in the junction of Shandong, Henan, Anhui and Jiangsu provinces, confirming that the crop residue burning was the dominant cause for the high AAOD.

The hourly estimated DRE from crop residue burning at TOA reached a maximum of $+22.66 \text{ W m}^{-2}$ at the Suixi site. On average, during the harvest period, crop residue burning introduced a positive DRE of $+0.14 \text{ W m}^{-2}$ throughout East China, which was higher than the cooling-to-neutral DRE estimates of open biomass burning in previous studies. BC was the leading absorptive component in crop-residue-burning-sourced aerosols and introduced an averaged DRE of $+0.79 \text{ W m}^{-2}$, while OA from crop burning brought about a net negative DRE (-0.22 W m^{-2}) at TOA. The negative DRE of OA scattering (-0.43 W m^{-2}) was roughly twice the magnitude of positive DRE of OA. The consideration of OA absorption therefore reduced the negative OA DRE estimates from crop burning by half, making the net DRE estimates of crop residue burning more positive. Higher absolute values of BC DRE ($> +2.0 \text{ W m}^{-2}$) and OA DRE ($< -0.2 \text{ W m}^{-2}$) from crop residue burning during the harvest season were mainly concentrated in the North China Plain, following a similar spatial distribution to the modelled AAOD. Sensitivity tests showed that the DRE of OA absorption strongly depended on the absorptivity and BC-to-OA ratio from crop residue burning and that using volume mixing treatment results in a higher positive DRE compared to the core–shell treatment. Several uncertainties remain regarding the estimated DRE in this study, due to the mixing state and morphology of the particles, burning conditions and emission inventory. Aerosol–radiation interactions due to carbonaceous aerosol from crop residue burning in the summer harvest might bring further effects on planetary boundary layer meteorology, turbulent kinetic energy, clouds and precipitation (Liu et al., 2016; Huang et al., 2016; Wilcox et al., 2016). Continued investigation of the mixing manner and ratio of biomass burning aerosol, their morphology and optical properties, their variation during the atmospheric aging processes, and their further impacts on clouds, transport and regional climate is still required. The BC mixing state and associated absorption enhancement based on coating thickness from BC aging processes will be treated in detail in future studies.

Data availability. The MODIS Level-2 Atmospheric Aerosol Product (04_L2) data can be accessed from https://modis-atmos.gsfc.nasa.gov/MOD04_L2/ (doi:10.5067/MODIS/MOD04_L2.006, Levy and Hsu, 2015). The ERA-Interim data can be accessed from <http://www.ecmwf.int/en/research/climate-reanalysis/era-interim> (ECMWF, 2011). Other data used in this study are available from the corresponding author upon request (songyu@pku.edu.cn).

The Supplement related to this article is available online at doi:10.5194/acp-17-5205-2017-supplement.

Competing interests. The authors declare that they have no conflict of interest.

Acknowledgements. The MODIS Level-2 Atmospheric Aerosol Product (04_L2) data were obtained from NASA L1 and Atmosphere Archive and Distribution System (LAADS), USA. The ERA-Interim data were provided by the European Centre for Medium-Range Weather Forecasts. This research was supported by the National Natural Science Foundation of China (41675142 and 41275155) and the NERC APHH AIRPRO project (NE/N00695X/1).

Edited by: L. Molina

Reviewed by: two anonymous referees

References

- Abel, S. J., Highwood, E. J., Haywood, J. M., and Stringer, M. A.: The direct radiative effect of biomass burning aerosols over southern Africa, *Atmos. Chem. Phys.*, 5, 1999–2018, doi:10.5194/acp-5-1999-2005, 2005.
- Ackerman, T. P. and Toon, O. B.: Absorption of visible radiation in atmosphere containing mixtures of absorbing and nonabsorbing particles, *Appl. Optics*, 20, 3661–3668, 1981.
- Adachi, K., Chung, S. H., and Buseck, P. R.: Shapes of soot aerosol particles and implications for their effects on climate, *J. Geophys. Res.-Atmos.*, 115, D15206, doi:10.1029/2009JD012868, 2010.
- Andreae, M. O. and Gelencsér, A.: Black carbon or brown carbon? The nature of light-absorbing carbonaceous aerosols, *Atmos. Chem. Phys.*, 6, 3131–3148, doi:10.5194/acp-6-3131-2006, 2006.
- Archer-Nicholls, S., Lowe, D., Schultz, D. M., and McFiggans, G.: Aerosol–radiation–cloud interactions in a regional coupled model: the effects of convective parameterisation and resolution, *Atmos. Chem. Phys.*, 16, 5573–5594, doi:10.5194/acp-16-5573-2016, 2016.
- Barnard, J. C., Fast, J. D., Paredes-Miranda, G., Arnott, W. P., and Laskin, A.: Technical Note: Evaluation of the WRF-Chem “Aerosol Chemical to Aerosol Optical Properties” Module using data from the MILAGRO campaign, *Atmos. Chem. Phys.*, 10, 7325–7340, doi:10.5194/acp-10-7325-2010, 2010.
- Bauer, S. E., Ault, A., and Prather, K. A.: Evaluation of aerosol mixing state classes in the GISS modelE-MATRIX climate model

- using single-particle mass spectrometry measurements, *J. Geophys. Res.-Atmos.*, 118, 9834–9844, doi:10.1002/jgrd.50700, 2013.
- Bond, T. C.: Spectral dependence of visible light absorption by carbonaceous particles emitted from coal combustion, *Geophys. Res. Lett.*, 28, 4075–4078, 2001.
- Bond, T. C., Streets, D. G., Yarber, K. F., Nelson, S. M., Woo, J., and Klimont, Z.: A technology-based global inventory of black and organic carbon emissions from combustion, *J. Geophys. Res.*, 109, D14203, doi:10.1029/2003JD003697, 2004.
- Bond, T. C., Habib, G., and Bergstrom, R. W.: Limitations in the enhancement of visible light absorption due to mixing state, *J. Geophys. Res.*, 111, D20211, doi:10.1029/2006JD007315, 2006.
- Bond, T. C., Doherty, S. J., Fahey, D. W., Forster, P. M., Berntsen, T., DeAngelo, B. J., Flanner, M. G., Ghan, S., Kärcher, B., Koch, D., Kinne, S., Kondo, Y., Quinn, P. K., Sarofim, M. C., Schultz, M. G., Schulz, M., Venkataraman, C., Zhang, H., Zhang, S., Bellouin, N., Guttikunda, S. K., Hopke, P. K., Jacobson, M. Z., Kaiser, J. W., Klimont, Z., Lohmann, U., Schwarz, J. P., Shindell, D., Storelvmo, T., Warren, S. G., and Zender, C. S.: Bounding the role of black carbon in the climate system: A scientific assessment, *J. Geophys. Res.-Atmos.*, 118, 5380–5552, doi:10.1002/jgrd.50171, 2013.
- Boucher, O. and Anderson, T. L.: General circulation model assessment of the sensitivity of direct climate forcing by anthropogenic sulfate aerosols to aerosol size and chemistry, *J. Geophys. Res.-Atmos.*, 100, 26117–26134, 1995.
- Cao, J., Zhu, C., Chow, J. C., Watson, J. G., Han, Y., Wang, G., Shen, Z., and An, Z.: Black carbon relationships with emissions and meteorology in Xi'an, China, *Atmos. Res.*, 94, 194–202, doi:10.1016/j.atmosres.2009.05.009, 2009.
- Chang, S. G., Brodzinsky, R., Gundel, L. A., and Novakov, T.: Chemical and Catalytic Properties of Elemental Carbon, in: Particulate Carbon: Atmospheric Life Cycle, edited by: Wolff, G. T. and Klimisch, R. L., Springer, US, 159–181, 1982.
- Chapman, E. G., Gustafson Jr., W. I., Easter, R. C., Barnard, J. C., Ghan, S. J., Pekour, M. S., and Fast, J. D.: Coupling aerosol-cloud-radiative processes in the WRF-Chem model: Investigating the radiative impact of elevated point sources, *Atmos. Chem. Phys.*, 9, 945–964, doi:10.5194/acp-9-945-2009, 2009.
- Chung, C. E., Ramanathan, V., and Decremer, D.: Observationally constrained estimates of carbonaceous aerosol radiative forcing, *P. Nat. Acad. Sci. USA*, 109, 11624–11629, doi:10.1073/pnas.1203707109, 2012.
- Dee, D. P., Uppala, S. M., Simmons, A. J., Berrisford, P., Poli, P., Kobayashi, S., Andrae, U., Balmaseda, M. A., Balsamo, G., Bauer, P., Bechtold, P., Beljaars, A. C. M., van de Berg, L., Bidlot, J., Bormann, N., Delsol, C., Dragani, R., Fuentes, M., Geer, A. J., Haimberger, L., Healy, S. B., Hersbach, H., Hölm, E. V., Isaksen, L., Källberg, P., Köhler, M., Matricardi, M., McNally, A. P., Monge-Sanz, B. M., Morcrette, J. J., Park, B. K., Peubey, C., de Rosnay, P., Tavolato, C., Thépaut, J. N., and Vitart, F.: The ERA-Interim reanalysis: configuration and performance of the data assimilation system, *Q. J. Roy. Meteor. Soc.*, 137, 553–597, doi:10.1002/qj.828, 2011.
- Dhammapala, R., Claiborn, C., Jimenez, J., Corkill, J., Gullett, B., Simpson, C., and Paulsen, M.: Emission factors of PAHs, methoxyphenols, levoglucosan, elemental carbon and organic carbon from simulated wheat and Kentucky bluegrass stubble burns, *Atmos. Environ.*, 41, 2660–2669, doi:10.1016/j.atmosenv.2006.11.023, 2007.
- ECMWF (European Centre for Medium-Range Weather Forecasts): ERA-Interim archive Version 2.0, available at: <http://www.ecmwf.int/en/research/climate-reanalysis/era-interim>, Reading, UK, 2011.
- Emmons, L. K., Walters, S., Hess, P. G., Lamarque, J.-F., Pfister, G. G., Fillmore, D., Granier, C., Guenther, A., Kinnison, D., Laepple, T., Orlando, J., Tie, X., Tyndall, G., Wiedinmyer, C., Baugheum, S. L., and Kloster, S.: Description and evaluation of the Model for Ozone and Related chemical Tracers, version 4 (MOZART-4), *Geosci. Model Dev.*, 3, 43–67, doi:10.5194/gmd-3-43-2010, 2010.
- Fast, J. D., Gustafson, W. I., Easter, R. C., Zaveri, R. A., Barnard, J. C., Chapman, E. G., Grell, G. A., and Peckham, S. E.: Evolution of ozone, particulates, and aerosol direct radiative forcing in the vicinity of Houston using a fully coupled meteorology-chemistry-aerosol model, *J. Geophys. Res.*, 111, D21305, doi:10.1029/2005JD006721, 2006.
- Feichter, J., Lohmann, U., and Schult, I.: The atmospheric sulfur cycle in ECHAM-4 and its impact on the shortwave radiation, *Clim. Dynam.*, 13, 235–246, 1997.
- Feng, Y., Ramanathan, V., and Kotamarthi, V. R.: Brown carbon: a significant atmospheric absorber of solar radiation?, *Atmos. Chem. Phys.*, 13, 8607–8621, doi:10.5194/acp-13-8607-2013, 2013.
- Fu, P. Q., Kawamura, K., Chen, J., Li, J., Sun, Y. L., Liu, Y., Tachibana, E., Aggarwal, S. G., Okuzawa, K., Tanimoto, H., Kanaya, Y., and Wang, Z. F.: Diurnal variations of organic molecular tracers and stable carbon isotopic composition in atmospheric aerosols over Mt. Tai in the North China Plain: an influence of biomass burning, *Atmos. Chem. Phys.*, 12, 8359–8375, doi:10.5194/acp-12-8359-2012, 2012.
- Gao, Y., Zhao, C., Liu, X., Zhang, M., and Leung, L. R.: WRF-Chem simulations of aerosols and anthropogenic aerosol radiative forcing in East Asia, *Atmos. Environ.*, 92, 250–266, doi:10.1016/j.atmosenv.2014.04.038, 2014.
- Ghan, S. J., Liu, X., Easter, R. C., Zaveri, R., Rasch, P. J., Yoon, J. H., and Eaton, B.: Toward a Minimal Representation of Aerosols in Climate Models: Comparative Decomposition of Aerosol Direct, Semidirect, and Indirect Radiative Forcing, *J. Climate*, 25, 6461–6476, doi:10.1175/JCLI-D-11-00650.1, 2012.
- Gilardoni, S., Liu, S., Takahama, S., Russell, L. M., Allan, J. D., Steinbrecher, R., Jimenez, J. L., De Carlo, P. F., Dunlea, E. J., and Baumgardner, D.: Characterization of organic ambient aerosol during MIRAGE 2006 on three platforms, *Atmos. Chem. Phys.*, 9, 5417–5432, doi:10.5194/acp-9-5417-2009, 2009.
- Grell, G. A., Peckham, S. E., Schmitz, R., McKeen, S. A., Frost, G., Skamarock, W. C., and Eder, B.: Fully coupled “online” chemistry within the WRF model, *Atmos. Environ.*, 39, 6957–6975, doi:10.1016/j.atmosenv.2005.04.027, 2005.
- Guenther, A., Karl, T., Harley, P., Wiedinmyer, C., Palmer, P. I., and Geron, C.: Estimates of global terrestrial isoprene emissions using MEGAN (Model of Emissions of Gases and Aerosols from Nature), *Atmos. Chem. Phys.*, 6, 3181–3210, doi:10.5194/acp-6-3181-2006, 2006.
- Hays, M. D., Fine, P. M., Geron, C. D., Kleeman, M. J., and Gullett, B. K.: Open burning of agricultural biomass: Physical and chem-

- ical properties of particle-phase emissions, *Atmos. Environ.*, 39, 6747–6764, doi:10.1016/j.atmosenv.2005.07.072, 2005.
- Heald, C. L., Ridley, D. A., Kroll, J. H., Barrett, S. R. H., Cady-Pereira, K. E., Alvarado, M. J., and Holmes, C. D.: Contrasting the direct radiative effect and direct radiative forcing of aerosols, *Atmos. Chem. Phys.*, 14, 5513–5527, doi:10.5194/acp-14-5513-2014, 2014.
- Hobbs, P. V., Reid, J. S., Kotchenruther, R. A., Ferek, R. J., and Weiss, R.: Direct radiative forcing by smoke from biomass burning, *Science*, 275, 1777–1778, 1997.
- Hsu, N. C., Tsay, S., King, M. D., and Herman, J. R.: Deep blue retrievals of Asian aerosol properties during ACE-Asia, *IEEE T. Geosci. Remote*, 44, 3180–3195, 2006.
- Huang, X., Li, M., Li, J., and Song, Y.: A high-resolution emission inventory of crop burning in fields in China based on MODIS Thermal Anomalies/Fire products, *Atmos. Environ.*, 50, 9–15, doi:10.1016/j.atmosenv.2012.01.017, 2012.
- Huang, X., Song, Y., Zhao, C., Cai, X., Zhang, H., and Zhu, T.: Direct radiative effect by multicomponent aerosol over China, *J. Climate*, 28, 3472–3495, doi:10.1175/JCLI-D-14-00365.1, 2015.
- Huang, X., Ding, A., Liu, L., Liu, Q., Ding, K., Niu, X., Nie, W., Xu, Z., Chi, X., Wang, M., Sun, J., Guo, W., and Fu, C.: Effects of aerosol-radiation interaction on precipitation during biomass-burning season in East China, *Atmos. Chem. Phys.*, 16, 10063–10082, doi:10.5194/acp-16-10063-2016, 2016.
- Jacobson, M. Z.: Isolating nitrated and aromatic aerosols and nitrated aromatic gases as sources of ultraviolet light absorption, *J. Geophys. Res.-Atmos.*, 104, 3527–3542, 1999.
- Jacobson, M. Z.: Strong radiative heating due to the mixing state of black carbon in atmospheric aerosols, *Nature*, 409, 695–697, 2001.
- Jacobson, M. Z.: Effects of biomass burning on climate, accounting for heat and moisture fluxes, black and brown carbon, and cloud absorption effects, *J. Geophys. Res.-Atmos.*, 119, 8980–9002, doi:10.1002/2014JD021861, 2014.
- Kirchstetter, T. W., Novakov, T., and Hobbs, P. V.: Evidence that the spectral dependence of light absorption by aerosols is affected by organic carbon, *J. Geophys. Res.-Atmos.*, 109, D21208, doi:10.1029/2004JD004999, 2004.
- Knote, C., Hodzic, A., Jimenez, J. L., Volkamer, R., Orlando, J. J., Baidar, S., Brioude, J., Fast, J., Gentner, D. R., Goldstein, A. H., Hayes, P. L., Knighton, W. B., Oetjen, H., Setyan, A., Stark, H., Thalman, R., Tyndall, G., Washenfelder, R., Waxman, E., and Zhang, Q.: Simulation of semi-explicit mechanisms of SOA formation from glyoxal in aerosol in a 3-D model, *Atmos. Chem. Phys.*, 14, 6213–6239, doi:10.5194/acp-14-6213-2014, 2014.
- Knote, C., Hodzic, A., and Jimenez, J. L.: The effect of dry and wet deposition of condensable vapors on secondary organic aerosols concentrations over the continental US, *Atmos. Chem. Phys.*, 15, 1–18, doi:10.5194/acp-15-1-2015, 2015.
- Kodros, J. K., Scott, C. E., Farina, S. C., Lee, Y. H., L'Orange, C., Volckens, J., and Pierce, J. R.: Uncertainties in global aerosols and climate effects due to biofuel emissions, *Atmos. Chem. Phys.*, 15, 8577–8596, doi:10.5194/acp-15-8577-2015, 2015.
- Kodros, J. K., Cucinotta, R., Ridley, D. A., Wiedinmyer, C., and Pierce, J. R.: The aerosol radiative effects of uncontrolled combustion of domestic waste, *Atmos. Chem. Phys.*, 16, 6771–6784, doi:10.5194/acp-16-6771-2016, 2016.
- Lack, D. A., Langridge, J. M., Bahreini, R., Cappa, C. D., Middelebrook, A. M., and Schwarz, J. P.: Brown carbon and internal mixing in biomass burning particles, *P. Natl. Acad. Sci.*, 109, 14802–14807, doi:10.1073/pnas.1206575109, 2012.
- Laskin, A., Laskin, J., and Nizkorodov, S. A.: Chemistry of Atmospheric Brown Carbon, *Chem. Rev.*, 115, 4335–4382, doi:10.1021/cr5006167, 2015.
- Levy, R. and Hsu, C.: MODIS Atmosphere L2 Aerosol Product, NASA MODIS Adaptive Processing System, available at: http://dx.doi.org/10.5067/MODIS/MOD04_L2.006, Goddard Space Flight Center, USA, 2015.
- Li, J., Song, Y., Mao, Y., Mao, Z., Wu, Y., Li, M., Huang, X., He, Q., and Hu, M.: Chemical characteristics and source apportionment of PM_{2.5} during the harvest season in eastern China's agricultural regions, *Atmos. Environ.*, 92, 442–448, doi:10.1016/j.atmosenv.2014.04.058, 2014.
- Li, K., Liao, H., Mao, Y., and Ridley, D. A.: Source sector and region contributions to concentration and direct radiative forcing of black carbon in China, *Atmos. Environ.*, 124, 351–366, doi:10.1016/j.atmosenv.2015.06.014, 2016.
- Li, M., Zhang, Q., Kurokawa, J.-I., Woo, J.-H., He, K., Lu, Z., Ohara, T., Song, Y., Streets, D. G., Carmichael, G. R., Cheng, Y., Hong, C., Huo, H., Jiang, X., Kang, S., Liu, F., Su, H., and Zheng, B.: MIX: a mosaic Asian anthropogenic emission inventory under the international collaboration framework of the MICS-Asia and HTAP, *Atmos. Chem. Phys.*, 17, 935–963, doi:10.5194/acp-17-935-2017, 2017.
- Li, X., Wang, S., Duan, L., Hao, J., Li, C., Chen, Y., and Yang, L.: Particulate and Trace Gas Emissions from Open Burning of Wheat Straw and Corn Stover in China, *Environ. Sci. Technol.*, 41, 6052–6058, doi:10.1021/es0705137, 2007.
- Liu, D., Whitehead, J., Alfara, M. R., Reyes-Villegas, E., Spracklen, D. V., Reddington, C. L., Kong, S., Williams, P. I., Ting, Y., Haslett, S., Taylor, J. W., Flynn, M. J., Morgan, W. T., McFiggans, G., Coe, H., and Allan, J. D.: Black-carbon absorption enhancement in the atmosphere determined by particle mixing state, *Nat. Geosci.*, 10, 184–188, doi:10.1038/ngeo2901, 2017.
- Liu, J., Bergin, M., Guo, H., King, L., Kotra, N., Edgerton, E., and Weber, R. J.: Size-resolved measurements of brown carbon in water and methanol extracts and estimates of their contribution to ambient fine-particle light absorption, *Atmos. Chem. Phys.*, 13, 12389–12404, doi:10.5194/acp-13-12389-2013, 2013.
- Liu, L., Huang, X., Ding, A., and Fu, C.: Dust-induced radiative feedbacks in north China: A dust storm episode modeling study using WRF-Chem, *Atmos. Environ.*, 129, 43–54, doi:10.1016/j.atmosenv.2016.01.019, 2016.
- Liu, M., Song, Y., Yao, H., Kang, Y., Li, M., Huang, X., and Hu, M.: Estimating emissions from agricultural fires in the North China Plain based on MODIS fire radiative power, *Atmos. Environ.*, 112, 326–334, doi:10.1016/j.atmosenv.2015.04.058, 2015.
- Lu, Z., Zhang, Q., and Streets, D. G.: Sulfur dioxide and primary carbonaceous aerosol emissions in China and India, 1996–2010, *Atmos. Chem. Phys.*, 11, 9839–9864, doi:10.5194/acp-11-9839-2011, 2011.
- Matsui, H., Koike, M., Kondo, Y., Moteki, N., Fast, J. D., and Zaveri, R. A.: Development and validation of a black carbon mixing state resolved three-dimensional model: Aging processes

- and radiative impact, *J. Geophys. Res.-Atmos.*, 118, 2304–2326, doi:10.1029/2012JD018446, 2013.
- Mlawer, E. J., Taubman, S. J., Brown, P. D., Iacono, M. J., and Clough, S. A.: Radiative transfer for inhomogeneous atmospheres: RRTM, a validated correlated – k model for the long-wave, *J. Geophys. Res.-Atmos.*, 102, 16663–16682, 1997.
- Myhre, G., Berglen, T. F., Johnsrud, M., Hoyle, C. R., Berntsen, T. K., Christopher, S. A., Fahey, D. W., Isaksen, I. S. A., Jones, T. A., Kahn, R. A., Loeb, N., Quinn, P., Remer, L., Schwarz, J. P., and Yttri, K. E.: Modelled radiative forcing of the direct aerosol effect with multi-observation evaluation, *Atmos. Chem. Phys.*, 9, 1365–1392, doi:10.5194/acp-9-1365-2009, 2009.
- Myhre, G., Samset, B. H., Schulz, M., Balkanski, Y., Bauer, S., Berntsen, T. K., Bian, H., Bellouin, N., Chin, M., Diehl, T., Easter, R. C., Feichter, J., Ghan, S. J., Hauglustaine, D., Iversen, T., Kinne, S., Kirkevåg, A., Lamarque, J.-F., Lin, G., Liu, X., Lund, M. T., Luo, G., Ma, X., van Noije, T., Penner, J. E., Rasch, P. J., Ruiz, A., Seland, Ø., Skeie, R. B., Stier, P., Takemura, T., Tsigaridis, K., Wang, P., Wang, Z., Xu, L., Yu, H., Yu, F., Yoon, J.-H., Zhang, K., Zhang, H., and Zhou, C.: Radiative forcing of the direct aerosol effect from AeroCom Phase II simulations, *Atmos. Chem. Phys.*, 13, 1853–1877, doi:10.5194/acp-13-1853-2013, 2013.
- Nordmann, S., Cheng, Y. F., Carmichael, G. R., Yu, M., Denier van der Gon, H. A. C., Zhang, Q., Saide, P. E., Pöschl, U., Su, H., Birmili, W., and Wiedensohler, A.: Atmospheric black carbon and warming effects influenced by the source and absorption enhancement in central Europe, *Atmos. Chem. Phys.*, 14, 12683–12699, doi:10.5194/acp-14-12683-2014, 2014.
- Park, R. J., Kim, M. J., Jeong, J. I., Youn, D., and Kim, S.: A contribution of brown carbon aerosol to the aerosol light absorption and its radiative forcing in East Asia, *Atmos. Environ.*, 44, 1414–1421, doi:10.1016/j.atmosev.2010.01.042, 2010.
- Peng, J., Hu, M., Guo, S., Du, Z., Zheng, J., Shang, D., Levy Zamora, M., Zeng, L., Shao, M., Wu, Y., Zheng, J., Wang, Y., Glen, C. R., Collins, D. R., Molina, M. J., and Zhang, R.: Markedly enhanced absorption and direct radiative forcing of black carbon under polluted urban environments, *P. Natl. Acad. Sci.*, 113, 4266–4271, doi:10.1073/pnas.1602310113, 2016.
- Ramanathan, V. and Carmichael, G.: Global and regional climate changes due to black carbon, *Nat. Geosci.*, 1, 221–227, doi:10.1038/ngeo156, 2008.
- Randerson, J. T., Chen, Y., van der Werf, G. R., Rogers, B. M., and Morton, D. C.: Global burned area and biomass burning emissions from small fires, *J. Geophys. Res.*, 117, G04012, doi:10.1029/2012JG002128, 2012.
- Roy, D. P., Boschetti, L., Justice, C. O., and Ju, J.: The collection 5 MODIS burned area product – Global evaluation by comparison with the MODIS active fire product, *Remote Sens. Environ.*, 112, 3690–3707, 2008.
- Sakaeda, N., Wood, R., and Rasch, P. J.: Direct and semidirect aerosol effects of southern African biomass burning aerosol, *J. Geophys. Res.*, 116, D12205, doi:10.1029/2010JD015540, 2011.
- Saleh, R., Robinson, E. S., Tkacik, D. S., Ahern, A. T., Liu, S., Aiken, A. C., Sullivan, R. C., Presto, A. A., Dubey, M. K., Yokelson, R. J., Donahue, N. M., and Robinson, A. L.: Brownness of organics in aerosols from biomass burning linked to their black carbon content, *Nat. Geosci.*, 7, 647–650, doi:10.1038/ngeo2220, 2014.
- Saleh, R., Marks, M., Heo, J., Adams, P. J., Donahue, N. M., and Robinson, A. L.: Contribution of brown carbon and lensing to the direct radiative effect of carbonaceous aerosols from biomass and biofuel burning emissions, *J. Geophys. Res.-Atmos.*, 120, 10285–10296, doi:10.1002/2015JD023697, 2015.
- Schnaiter, M., Linke, C., Möhler, O., Naumann, K. H., Saathoff, H., Wagner, R., Schurath, U., and Wehner, B.: Absorption amplification of black carbon internally mixed with secondary organic aerosol, *J. Geophys. Res.-Atmos.*, 110, D19204, doi:10.1029/2005JD006046, 2005.
- Schulz, M., Textor, C., Kinne, S., Balkanski, Y., Bauer, S., Berntsen, T., Berglen, T., Boucher, O., Dentener, F., Guibert, S., Isaksen, I. S. A., Iversen, T., Koch, D., Kirkevåg, A., Liu, X., Montanaro, V., Myhre, G., Penner, J. E., Pitari, G., Reddy, S., Seland, Ø., Stier, P., and Takemura, T.: Radiative forcing by aerosols as derived from the AeroCom present-day and pre-industrial simulations, *Atmos. Chem. Phys.*, 6, 5225–5246, doi:10.5194/acp-6-5225-2006, 2006.
- Schwarz, J. P., Gao, R. S., Spackman, J. R., Watts, L. A., Thomson, D. S., Fahey, D. W., Ryerson, T. B., Peischl, J., Holloway, J. S., Trainer, M., Frost, G. J., Baynard, T., Lack, D. A., de Gouw, J. A., Warneke, C., and Del Negro, L. A.: Measurement of the mixing state, mass, and optical size of individual black carbon particles in urban and biomass burning emissions, *Geophys. Res. Lett.*, 35, L13810, doi:10.1029/2008GL033968, 2008.
- Song, Y., Liu, B., Miao, W., Chang, D., and Zhang, Y.: Spatiotemporal variation in nonagricultural open fire emissions in China from 2000 to 2007, *Global Biogeochem. Cy.*, 23, GB2008, doi:10.1029/2008GB003344, 2009.
- Song, Y., Chang, D., Liu, B., Miao, W., Zhu, L., and Zhang, Y.: A new emission inventory for nonagricultural open fires in Asia from 2000 to 2009, *Environ. Res. Lett.*, 5, 14014, doi:10.1088/1748-9326/5/1/014014, 2010.
- Stocker, T. F.: Climate change 2013: the physical science basis: Working Group I contribution to the Fifth assessment report of the Intergovernmental Panel on Climate Change, Cambridge University Press, 2014.
- Turn, S. Q., Jenkins, B. M., Chow, J. C., Pritchett, L. C., Campbell, D., Cahill, T., and Whalen, S. A.: Elemental characterization of particulate matter emitted from biomass burning: Wind tunnel derived source profiles for herbaceous and wood fuels, *J. Geophys. Res.-Atmos.*, 102, 3683–3699, 1997.
- Wang, Q., Huang, R., Cao, J., Han, Y., Wang, G., Li, G., Wang, Y., Dai, W., Zhang, R., and Zhou, Y.: Mixing state of black carbon aerosol in a heavily polluted urban area of China: Implications for light absorption enhancement, *Aerosol Sci. Tech.*, 48, 689–697, 2014.
- Wang, X., Heald, C. L., Ridley, D. A., Schwarz, J. P., Spackman, J. R., Perring, A. E., Coe, H., Liu, D., and Clarke, A. D.: Exploiting simultaneous observational constraints on mass and absorption to estimate the global direct radiative forcing of black carbon and brown carbon, *Atmos. Chem. Phys.*, 14, 10989–11010, doi:10.5194/acp-14-10989-2014, 2014.
- Wilcox, E. M., Thomas, R. M., Praveen, P. S., Pistone, K., Bender, F. A. M., and Ramanathan, V.: Black carbon solar absorption suppresses turbulence in the atmospheric boundary layer, *P. Natl. Acad. Sci. USA*, 113, 11794–11799, doi:10.1073/pnas.1525746113, 2016.

- Xia, X., Li, Z., Holben, B., Wang, P., Eck, T., Chen, H., Cribb, M., and Zhao, Y.: Aerosol optical properties and radiative effects in the Yangtze Delta region of China, *J. Geophys. Res.*, 112, D22S12, doi:10.1029/2007JD008859, 2007.
- Yamaji, K., Li, J., Uno, I., Kanaya, Y., Irie, H., Takigawa, M., Komazaki, Y., Pochanart, P., Liu, Y., Tanimoto, H., Ohara, T., Yan, X., Wang, Z., and Akimoto, H.: Impact of open crop residual burning on air quality over Central Eastern China during the Mount Tai Experiment 2006 (MTX2006), *Atmos. Chem. Phys.*, 10, 7353–7368, doi:10.5194/acp-10-7353-2010, 2010.
- Yang, S., He, H., Lu, S., Chen, D., and Zhu, J.: Quantification of crop residue burning in the field and its influence on ambient air quality in Suqian, China, *Atmos. Environ.*, 42, 1961–1969, doi:10.1016/j.atmosenv.2007.12.007, 2008.
- Yoon, S. and Kim, J.: Influences of relative humidity on aerosol optical properties and aerosol radiative forcing during ACE-Asia, *Atmos. Environ.*, 40, 4328–4338, 2006.
- Zaveri, R. A., Easter, R. C., Fast, J. D., and Peters, L. K.: Model for Simulating Aerosol Interactions and Chemistry (MOSAIC), *J. Geophys. Res.*, 113, D13204, doi:10.1029/2007JD008782, 2008.
- Zhang, H., Ye, X., Cheng, T., Chen, J., Yang, X., Wang, L., and Zhang, R.: A laboratory study of agricultural crop residue combustion in China: Emission factors and emission inventory, *Atmos. Environ.*, 42, 8432–8441, doi:10.1016/j.atmosenv.2008.08.015, 2008.
- Zhang, X., Lin, Y., Surratt, J. D., and Weber, R. J.: Sources, composition and absorption Ångstrom exponent of light-absorbing organic components in aerosol extracts from the Los Angeles Basin, *Environ. Sci. Technol.*, 47, 3685–3693, 2013.
- Zhang, Y.: Online-coupled meteorology and chemistry models: history, current status, and outlook, *Atmos. Chem. Phys.*, 8, 2895–2932, doi:10.5194/acp-8-2895-2008, 2008.
- Zhao, C., Ruby Leung, L., Easter, R., Hand, J., and Avise, J.: Characterization of speciated aerosol direct radiative forcing over California, *J. Geophys. Res.-Atmos.*, 118, 2372–2388, doi:10.1029/2012JD018364, 2013.
- Zhou, Y., Xing, X., Lang, J., Chen, D., Cheng, S., Wei, L., Wei, X., and Liu, C.: A comprehensive biomass burning emission inventory with high spatial and temporal resolution in China, *Atmos. Chem. Phys.*, 17, 2839–2864, doi:10.5194/acp-17-2839-2017, 2017.
- Zhuang, B., Jiang, F., Wang, T., Li, S., and Zhu, B.: Investigation on the direct radiative effect of fossil fuel black-carbon aerosol over China, *Theor. Appl. Climatol.*, 104, 301–312, 2011.